Water Evaporation and Condensation in Air With Radiation: The Self-Similar Spalding Model

M. Q. Brewster
Department of Mechanical Science and Engineering,
University of Illinois,
Urbana, IL 61801
e-mail: brewster@illinois.edu

Several simple ways of improving the accuracy of Spalding model predictions over common textbook conventions for air/water evaporation/condensation problems are illustrated using open-literature examples. First is the choice of thermodynamic reference state for enthalpy evaluation. The common practice of choosing the steam table reference point (0.01 °C) with water-vapor enthalpy of h_{fg} (2501 kJ/kg) and air enthalpy of zero introduces an enthalpy mismatch between air and water vapor that unnecessarily compromises accuracy. Choosing the air/water interface temperature as the reference point and setting both air and water-vapor enthalpies at this point to the same numerical value gives the most accurate results of several methods tried. Second is judicious choice of the blowing factor in high-rate mass transfer situations. The laminar boundary layer blowing factor is more accurate than the common stagnant-film (Couette flow) blowing factor for flat-plate flow and may be more accurate for a cylinder in crossflow under laminar conditions, as illustrated by the example of air leak effect on steam condenser tube performance. Third is radiation modeling, often a problematic or ignored feature in this type of problem. Two common, but opposite, assumptions about radiation participation in water—transparent interface and opaque interface—are shown to be equivalent for most purposes. A methodology is introduced for modeling true interfacial absorption/emission associated with phase change if/when the amount of this effect becomes known well enough to justify its inclusion. The importance of including radiation is illustrated by several examples: cloud droplet evaporation–condensation, sweat cooling, and the wet-bulb psychrometer. Fourth is inaccuracy introduced by unnecessarily setting Lewis number to unity. [DOI: 10.1115/1.4036075]

Keywords: Spalding formulation, air–water, condensation, evaporation, radiation

1 Introduction—"In Theory There is no Difference Between Theory and Practice"

There are many industrially and geophysically important processes that involve evaporation and condensation of water in the presence of air, from drying and evaporative cooling to cloud formation and stability. The self-similar Spalding theory of heat and mass transfer [1] applied to a two-phase, binary system with one transferred substance (water) is the classic textbook model [2–4] of these processes. Yet in spite of the relative simplicity of this popular theory, there are several practices that persist, even in current textbooks, which unnecessarily compromise accuracy of results. Spalding's theory and its application to air/water provide a perfect example of the Yogi Berra maxim: "In theory, there is no difference between theory and practice. In practice there is."

While it is recognized that there is always some difference between theory and practice, or between theory and experiment, due to limiting theoretical assumptions, the number of discrepancies, which exists between Spalding's theory and its application to air/water, even in standard textbooks, is far more than need be. At the same time, it is recognized that in real-world design there are multiple competing sources of uncertainty or error, and that analysis error is just one of those. This fact might be used to justify reduced-accuracy approximations in applying Spalding theory to air/water, such as Lewis number unity or Couette flow (stagnant film) blowing factor. However, there are many situations, as demonstrated with four specific examples below, where analysis accuracy has suffered unnecessarily by the use of such approximations. In particular, there is a widespread source of systematic error associated with the thermodynamic reference state choice for enthalpy that has not been recognized in the open literature.

The main purpose of this communication is to point out, using textbook analyses and examples, a few simple ways in which classical, self-similar Spalding heat and mass transfer theory can be applied with greater accuracy to problems involving water evaporating or condensing in the presence of air. A secondary purpose is to include radiation in a more general way than has been done before—allowing for interfacial absorption, interfacial emission, volumetric absorption, and volumetric emission—and to clarify further the physical and mathematical issues around modeling these various sources and sinks of radiation.

2 Analysis

2.1 Spalding Model. The Spalding model describes evaporation or condensation of a volatile substance in the presence of a vapor mixture, typically air. The model is centered on mass and energy balances at the interface between the condensed phase and vapor phase, as shown in Fig. 1. The condensed phase is pure species-1, e.g., liquid water, and the vapor phase is a binary ideal gas mixture of condensable vapor (species-1), e.g., water vapor, and noncondensable gas (species-2), e.g., dry air. The water can be either evaporating with positive mass flux ($\dot{m}'' > 0$, flux arrows as in Fig. 1) or condensing ($\dot{m}'' < 0$, arrows opposite those in

Contributed by the Heat Transfer Division of ASME for publication in the Journal of Heat Transfer. Manuscript received August 23, 2016; final manuscript received February 17, 2017; published online April 11, 2017. Assoc. Editor: Amitabh Narain.

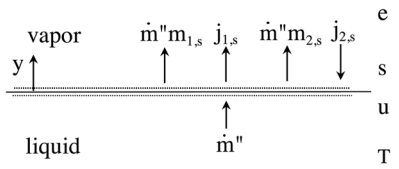

Fig. 1 Thermodynamic state definitions and mass fluxes at water vapor–liquid interface

Fig. 1). Self-similarity of water-vapor mass fraction m_1 and mixture enthalpy h in the governing equations is used to enable a generalized solution, as described below.

The interfacial mass balance corresponding to Fig. 1 ($\dot{m}'' > 0$, evaporation) indicates that the mass flux of water approaching the interface as liquid from below equals the sum of the diffusive and convective mass fluxes of water vapor above and away from the interface

$$\dot{m}'' = \overbrace{-\rho D_{12}\frac{\partial m_1}{\partial y}\bigg|_s}^{j_{1,s}} + \dot{m}'' m_{1,s} \tag{1}$$

In Eq. (1), only terms involving species-1 appear because there is no net transport of species-2 (which is insoluble in the condensed phase of species-1). The air (species-2) mass fluxes by convection and diffusion are equal and opposite: $\dot{m}'' m_{2,s} = -j_{2,s}$. That is, the rate of upward convection of air with the bulk flow (at the mass-averaged vapor velocity) equals the rate of downward diffusion of air. In addition, the diffusion fluxes of species-1 and species-2 are equal and opposite, $-j_{2,s} = j_{1,s}$, by definition of mass-average (bulk) velocity. As a result, there is equality in magnitude of three species-specific mass fluxes on the vapor side of the interface: $m_{2,s}\dot{m}'' = -j_{2,s} = j_{1,s}$.

The interfacial energy balance, shown schematically in Fig. 2 (for evaporation, $\dot{m}'' > 0$), indicates that the heat required to raise the enthalpy of the flow from the liquid value (h_u) to the vapor mixture value (h_s) can be supplied by conduction from the liquid side ($q_{c,u}$) and/or from the gas side $\left(q_{c,s} = -k\frac{\partial T}{\partial y}\bigg|_s\right)$. It can also be supplied by radiation absorption from the gas side ($q_{r,s}$) (further elaboration of radiation is given below)

$$q_{c,u} + q_{r,s} + \dot{m}'' h_u = q_{c,s} + j_{i,s}h_{i,s} + \dot{m}'' h_s \tag{2}$$

The molecular diffusion enthalpy flux $j_{i,s}h_{i,s}$ (using Einstein summation notation and magnitude equality of the three mass fluxes noted above) is

$$j_{i,s}h_{i,s} = \sum_{i=1,2} j_{i,s}h_{i,s} = j_{1,s}(h_{1,s} - h_{2,s}) = m_{2,s}\dot{m}''(h_{1,s} - h_{2,s}) \tag{3}$$

The combined molecular diffusion energy flux on the vapor side of the interface (right-hand side of Eq. (2)) consists of both Fourier heat conduction ($q_{c,s}$) and species-based enthalpy diffusion, as given in Eq. (3). This combined flux is manipulated algebraically and then approximated in the Spalding model as follows:

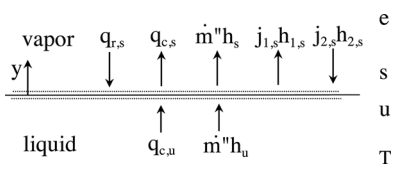

Fig. 2 Energy fluxes at water vapor–liquid interface with grouping by flux type

$$q_{c,s} + j_{i,s}h_{i,s} = -\rho\alpha\frac{\partial h}{\partial y}\bigg|_s + \underbrace{j_{1,s}(h_{1,s} - h_{2,s})}_{j_{i,s}h_{i,s}}\left(1 - \frac{1}{Le}\right) \simeq -\rho\alpha\frac{\partial h}{\partial y}\bigg|_s \tag{4}$$

The combined molecular flux is here written as the sum of mixture enthalpy gradient and a triple-product term comprised of the product of diffusion mass flux of species-1 ($j_{1,s}$), enthalpy difference between species-1 and species-2 ($h_{1,s} - h_{2,s}$), and a Lewis number-unity deviation factor ($1 - (1/Le)$). This triple-product term represents a small fraction of the $j_{i,s}h_{i,s}$ energy transport flux by species diffusion; "small" because $(1 - (1/Le)) \ll 1$ with $Le \sim 1$. Using the approximation that drops the triple-product term, the interface energy equation becomes

$$q_{c,u} + q_{r,s} + \dot{m}'' h_u \simeq -\rho\alpha\frac{\partial h}{\partial y}\bigg|_s + \dot{m}'' h_s \tag{5}$$

The interface energy equation, Eq. (5), and mass equation, Eq. (1), are now similar, as can be made more evident with Spalding's regrouping of terms and definitions of B-numbers and g-conductances. The B-numbers are defined so as to contain information about the thermodynamic driving potentials of the problem while the g-conductances contain information about the fluid mechanics and transport rates of the problem

$$\dot{m}'' = g_{m,h}B_{m,h} \tag{6}$$

$$B_m \equiv \frac{m_{1,s} - m_{1,e}}{1 - m_{1,s}}; \quad B_h \equiv \frac{h_s - h_e}{\left(h_u + \frac{q_{c,u} + q_{r,s}}{\dot{m}''}\right) - h_s} \tag{7}$$

$$g_m \equiv \frac{-\rho D_{12}}{(m_{1,s} - m_{1,e})}\frac{\partial m_1}{\partial y}\bigg|_s; \quad g_h \equiv \frac{-\rho\alpha}{(h_s - h_e)}\frac{\partial h}{\partial y}\bigg|_s \tag{8}$$

For complete similarity, the governing field equations and other boundary conditions must be similar, not just the interface conditions. This is illustrated next with governing equations for a two-dimensional boundary-layer type of flow.

For a steady, two-dimensional, constant-property flow with boundary layer approximations (e.g., negligible x-diffusion of mass, momentum, and energy), the species equation is

$$u\frac{\partial m_1}{\partial x} + v\frac{\partial m_1}{\partial y} = D_{12}\frac{\partial^2 m_1}{\partial y^2} \tag{9}$$

where u and v are the bulk (mass-average) velocity components. The energy equation is

$$u\frac{\partial h}{\partial x} + v\frac{\partial h}{\partial y} = \frac{\partial}{\partial y}\left[-j_i h_i + \frac{k}{C_p}\frac{\partial T}{\partial y}\right] \tag{10}$$

Introducing the same approximation for molecular energy flux

$$-k\frac{\partial T}{\partial y} + j_i h_i = -\rho\alpha\frac{\partial h}{\partial y} + \underbrace{j_1(h_1 - h_2)}_{j_i h_i}\left(1 - \frac{1}{Le}\right) \doteq -\rho\alpha\frac{\partial h}{\partial y} \tag{11}$$

the energy equation becomes

$$u\frac{\partial h}{\partial x} + v\frac{\partial h}{\partial y} = \alpha\frac{\partial^2 h}{\partial y^2} \tag{12}$$

in similitude with the species equation, Eq. (9). Solution of these equations, in conjunction with a similar momentum equation, gives the flow-specific conductance factors, g* and g/g*.

The g-terms effectively represent the gradients of species concentration and energy quantities at the s-surface. This information

is typically represented as a limiting solution for g in the low mass-transfer rate limit (g*), with a correction term for the effect of blowing on the velocity, species, and temperature or enthalpy profiles, (g/g*). The energy solution (g_h^*) is often cast in various other forms using common nondimensional parameters from convective heat transfer theory without mass transfer such as Nusselt number, Stanton number (if forced convection is involved), Colburn j-factor, etc.

$$g_h^* = \frac{\rho\alpha}{L} Nu_L \tag{13}$$

Here, L is a characteristic length-scale for the problem (e.g., stagnant film thickness in Stefan/Couette flow, droplet radius or diameter, length along a flat surface, etc.) The species solution (g_m^*) can similarly be written in terms of Sherwood number

$$g_m^* = \frac{\rho D_{12}}{L} Sh_L \tag{14}$$

The blowing/suction correction factor (g/g*) depends on the specific flow type. Exact solutions have been obtained for only a few flows such as Stefan flow (stagnant film), Couette flow, spherically symmetric droplet, uniform-velocity forced convection laminar boundary layer on an isothermal flat surface, and laminar natural convection boundary layer on an isothermal vertical flat plate. Stefan flow, Couette flow, and the spherically symmetric droplet problem give rise to the same correction factor

$$\left(\frac{g}{g^*}\right)_{m.h} = \frac{\ln(1+B_{m.h})}{B_{m.h}};\ (\text{Stagnant Film} - \text{Stefan/Couette/Droplet}) \tag{15}$$

This correction factor is often used in the absence of a g/g* solution for a more complicated flow, for example, in turbulent boundary layers. Sometimes the Stefan/Couette blowing factor is reasonably accurate for flows other than those for which it is derived, but not always.

The Spalding assumption to drop the triple-product term $j_1(h_1 - h_2)(1 - (1/Le))$ in the energy equation and interface conditions via Eqs. (11) and (4) can be justified a number of ways; nine ways are outlined in the original Spalding paper [1], covering both reacting and nonreacting systems. The most common justifications cited in the nonreacting, binary air/water system are Lewis number near unity ($Le \sim 1$) and/or "low" (diffusion-dominated/dilute) mass-transfer rate. *However, this term can also be made small by appropriate choice of enthalpy references such that the enthalpy difference factor is also made as small as possible.* The latter approach is typically not implemented in the literature. Based on the fact that the choice of energy reference is arbitrary thermodynamically as long as there are no chemical reactions, most texts [2,3,5] choose conventional enthalpy reference states that do not minimize the molecular diffusion energy flux term. Below we remedy that situation and discuss the impact of the energy reference choice. But next we introduce an alternative form of the interface energy equation.

2.2 Interface Energy Equation—Species Grouping. The energy equation can be written with different forms, depending on the type of terms that are grouped, and this difference plays a key role in the Spalding model. The Spalding model uses a flux-type grouping of terms, i.e., diffusive, $j_{i,s}h_{i,s}$, versus bulk-flow advective, $\dot{m}''h$. This grouping enables the key approximation that leads to the similarity of m_1 and h. In contrast, energy terms may also be grouped based on species type. Species grouping of energy at the interface is written as

$$q_{c,u} + q_{r,s} = q_{c,s} + \dot{m}'' h_{fg,s} \tag{16}$$

as illustrated in Fig. 3 (for $\dot{m}'' > 0$). In the species-grouped energy equation, the only enthalpy flux term that appears ($\dot{m}'' h_{fg,s}$) is the

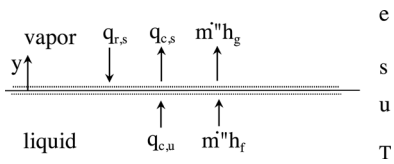

Fig. 3 Energy fluxes at water vapor–liquid interface with grouping by species type

latent enthalpy associated with the transferred species, species-1 (water). As in the mass equation, Eq. (1), this is because there is no net mass transport of species-2 (air), i.e., $j_{2,s} + m_{2,s}\,\dot{m}'' = 0$; therefore, there is no enthalpy flux by species-2, i.e., $(j_{2,s} + m_{2,s}\,\dot{m}'')h_{2,s} = 0$. Species-2 only contributes as a thermal conducting species via vapor mixture conductivity k in $q_{c,s}$. It should be noted that Eqs. (2) (species grouping) and (16) (flux grouping) are equivalent, i.e., the same equation, as can be shown algebraically using the definition of mixture enthalpy h, etc. It is also important to realize that this equation is not the one actually solved in the Spalding model. Nevertheless, it is still a valid equation and can be used to evaluate the conductive heat flux $q_{c,s}$ after the Spalding equations have been solved

$$q_{c,s} = q_{c,u} + q_{r,s} - \begin{cases} [\dot{m}''(h_s - h_u) + j_{i,s}h_{i,s}], & \text{flux grouping} \\ \dot{m}'' h_{fg,s}, & \text{species grouping} \end{cases} \tag{17}$$

2.3 Radiation Treatment: Volumetric Versus Interfacial. Radiation is a problematic—often ignored—aspect in problems involving water evaporation or condensation in air. Radiation is often justifiably neglected but it is also often ignored when it is not negligible. Some confusion about how to include radiation analytically probably exists because two opposite conventions/assumptions about the volumetric versus interfacial character of radiation in water/air systems have come into common use. Here, we seek to address that issue and propose a methodology for including both volumetric and interfacial radiation—so far as is presently possible—in the Spalding model framework.

Classically, absorption and emission of radiation require volume; a vanishingly thin (of molecular thickness) interface cannot absorb or emit an appreciable amount radiation, it is generally thought. This convention, which could be called the transparent interface convention, is the one adopted in Refs. [2] and [4]. However, in mathematical modeling, the assumption of surface or interfacial absorption/emission is often made, particularly for a relatively infrared-opaque material like water where the length-scale for emission and infrared absorption is often much smaller than other thermal transport length-scales. This opaque interface convention is adopted in Ref. [3]. Whether one convention or the other is more correct in any situation, or whether some intermediate treatment, such as a partially transparent-partially opaque interface, is needed are questions that undoubtedly add confusion to the issue of including radiation in a modeling analysis.

The above interface energy equations include a radiation term $q_{r,s}$; this is the net *interfacially* absorbed radiation flux (net absorbed = absorbed − emitted). In order to allow the possibility of both volumetric and interfacial radiation emission/absorption, we allow $q_{r,s}$ to be some fraction (f_s) of the total (= volumetric + interfacial) net absorbed radiation ($-q_r$), by defining

$$q_{r,s} = -f_s q_r \tag{18}$$

In addition to introducing the parameter f_s, Eq. (18) also introduces an arbitrary sign change that defines q_r as the total, net *emitted* (not absorbed) radiant flux from the liquid water into the vapor phase (net emitted = emitted − absorbed)

$$q_r = q_{r,em} - q_{r,ab} \tag{19}$$

Next, we introduce notation to allow the possibility that the fraction of interfacially absorbed radiation ($f_{s,ab}$) might be different from the fraction of interfacially emitted radiation ($f_{s,em}$)

$$f_s = \frac{f_{s,em}q_{r,em} - f_{s,ab}q_{r,ab}}{q_{r,em} - q_{r,ab}} \tag{20}$$

The interfacial energy equation (species grouping) can now be written as

$$q_{c,u} + f_{s,ab}q_{r,ab} = q_{c,s} + f_{s,em}q_{r,em} + \dot{m}''h_{fg,s} \tag{21}$$

Equation (21) allows that some fraction ($f_{s,ab}$) of the absorbed radiation from the vapor side ($q_{r,ab}$) can be absorbed in the interface and some fraction ($f_{s,em}$) of the radiation that is emitted to the vapor ($q_{r,em}$) can be emitted from the interface. While $f_{s,ab}$ and $f_{s,em}$ are considered to be zero classically from a physical point of view, and treating them otherwise (e.g., as one) has only been done for infrared modeling convenience, one may also consider $f_{s,ab} > 0$ or $f_{s,em} > 0$ for another reason: the intriguing possibility of phase-change radiation, radiation absorbed or emitted at the interface in concurrence with simultaneous phase change [6]. Not much is yet known about how to quantify $f_{s,ab}$ and $f_{s,em}$ for phase-change radiation. They are certainly spectrally dependent properties that could be integrated to define total properties. These total properties would depend on the interface temperature and the spectral distribution of the incident radiation, and would not necessarily be equal to each other. Initial studies [6] have suggested that phase-change radiation might be most active in the 5–10 μm spectral region, where $f_{s,ab}$ and $f_{s,em}$ are probably a few percent in magnitude, but more study is needed.

Note that if both $f_{s,ab}$ and $f_{s,em}$ are assumed to be zero (transparent interface) [2,4], so is f_s. If both $f_{s,ab}$ and $f_{s,em}$ are assumed to be one (opaque interface) [3], so is f_s. If some other combination of $f_{s,ab}$ and $f_{s,em}$ is assumed, f_s could be negative or even greater than one; it loses simple meaning as a fraction of something. In the examples discussed below, $f_{s,em}$, $f_{s,ab}$, and f_s will all be taken as either zero or one. It is shown below (see T-State and Tu-layer) that this choice has no impact on most of the outcomes predicted by the model.

2.4 Transport Properties. The Spalding model assumes constant density and transport properties. Various schemes for evaluating these properties have been proposed, such as the $^1/_2$ rule (arithmetic average or halfway between T_s and T_e). Mills observes [3] that a 1/3 rule is actually more accurate than the $^1/_2$ rule. Here, that issue is not investigated. Transport properties (and density) used in the examples below generally follow the $^1/_2$ rule, but when deviation from the $^1/_2$ rule occurs, the same properties are used as cited in the literature for that example.

2.5 Enthalpy Reference State. The thermodynamic reference state for a simple, compressible pure substance is usually viewed as the state where energy (either internal energy or enthalpy) is set to be zero. Here, the reference state will mean the state where enthalpy is chosen to be a specific value, not necessarily zero. When two species are involved in a nonreacting mixture, the choice of reference state for each species is independent and arbitrary (thermodynamically). Usually a pure substance requires two independent, intensive properties (e.g., temperature and pressure for single phase) to uniquely specify a state. In this paper, temperature alone will be sufficient to specify the reference state. This is because only enthalpies of incompressible liquid or ideal gas states are evaluated, which are functions of temperature alone. Entropy and free energy (which would require pressure too) are not evaluated. Relative enthalpies (sensible enthalpy changes) are evaluated using temperature integrals of specific heat. For liquid water, constant specific heat (C = 4.2 kJ/kg K) is assumed. For ideal gas states, fourth-order polynomial curve-fits for temperature-dependent specific heat are used [7]. Common choices for reference state temperature are the triple point of water ($T_{tp} = 0.01 \simeq 0\,^\circ$C) and the liquid–vapor interface temperature T_s. As noted above, the most common choice for reference enthalpy is zero. Another natural choice for the air/water system is the latent heat of water, h_{fg}, typically evaluated at the reference temperature, e.g., either 0 °C ($h_{fg,0} = 2501$ kJ/kg), or T_s ($h_{fg,s}$). Here we consider three reference systems, one that does not match vapor-phase enthalpies between species (A) and two that do (B and C). A shorthand notation for designating each reference system is a set of three numbers corresponding to the reference temperature T_{ref} in (°C), and the vapor enthalpies $h_{i,ref}$ in (kJ/kg), that is, $[T_{ref}, h_{1,ref}, h_{2,ref}]$.

2.5.1 Reference-A [0, 2501, 0] = [T_{tp}, $h_{fg,0}$, 0]. This reference system uses the common steam table reference for water, the triple point (0.01 ≃ 0 °C), with zero internal energy (and effectively zero enthalpy) for saturated liquid at this temperature. For air, the reference enthalpy is selected to be zero. This is a common reference choice in the literature [2,3,5] because it allows the use of steam tables while simplifying the algebra of approximate property evaluation expressions; however, it causes the vapor-phase enthalpies of air and water to be severely mismatched numerically, since the water vapor enthalpy at the reference temperature is $h_{fg}(T_{tp}) = h_{fg,0} = 2501$ kJ/kg.

2.5.2 Reference-B [0, 2501, 2501] = [T_{tp}, $h_{fg,0}$, $h_{fg,0}$]. This system also uses the triple point of water (0.01 ≃ 0 °C) with zero enthalpy for saturated liquid at this temperature. However, for air, the reference enthalpy at this temperature is also set to be 2501 kJ/kg, the same as for water vapor. This choice allows steam tables to be used for water properties, if desired, but more importantly causes the vapor enthalpies of water and air to be much more closely matched than with Reference-A.

2.5.3 Reference-C [T_s, 0, 0]. This system uses as a reference state the interface temperature T_s and sets both air and water vapor enthalpies to be zero at this temperature. By this choice, the vapor-phase enthalpies are nearly matched, as in Reference-B. This choice causes liquid water enthalpy at T_s to be negative, specifically $-h_{fg,s}$, and does not allow the use of steam tables for water properties. On the other hand, it simplifies some expressions by setting $h_{i,s} = h_s = 0$; for example, $j_{i,s}h_{i,s} = 0$.

2.6 T-State and Tu-Layer. The T-state is a thermodynamic state, either hypothetical or real, in the liquid (see Figs. 1–3). Physical T-states occur most often in the case of evaporative cooling, i.e., water supplied to the interface, not condensation. The T-state is defined as the state that would exist upstream of (below) the u-state if the region between the T- and u-states were governed by one-dimensional convection of liquid water and conduction (diffusion) of heat without chemical reaction, i.e., a one-dimensional, convective–diffusive balance.

The energy balance on the Tu-layer (the region between the T- and u-states) is

$$\dot{m}''h_T = \dot{m}''h_u + q_{c,u} + (1 - f_s)q_r \tag{22}$$

Recall that a fraction (or multiple) of q_r ($f_s q_r$) is allowed to originate from the interface such that the remainder ($1 - f_s$) originates from the Tu-layer. The T-state, then, if it is physical, represents the state of the water supplied to the interface, "far" from the interface, at a location below the interface where there are no gradients, e.g., no heat flux, only convective mass flux of water. Because of the relatively high thermal conductivity and diffusivity of water and the associated long thermal diffusive length scale (e.g., meters) in the liquid region, the T-state is often not realizable, only hypothetical. A situation in which the T-state is physically realizable is the adiabatic Tu-layer, wherein the net heat flux at the

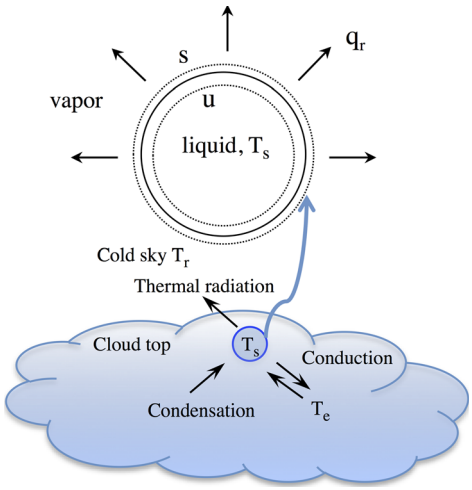

Fig. 4 Schematic diagram of Ex1: cloud droplet with radiation; detail for individual droplet residing near top of cloud shown above cloud

u-surface (sum of conduction and radiation) is zero ($q_{c,u} = -(1 - f_s)q_r$), such that the u- and T-states are identical ($h_T = h_u$, $T_T = T_s$).

Introducing the Tu-layer energy balance into the definition of B_h results in an alternative form for B_h

$$B_h = \frac{h_e - h_s}{h_s - \left(h_T - \dfrac{q_r}{\dot{m}''}\right)} \tag{23}$$

which shows that the mass transfer rate and interface temperature (if it is an unknown) are not influenced by the assumed value of f_s. Hence, the choice of f_s is arbitrary as far as most important outcomes are concerned. Its value only affects the temperature profile in the liquid phase, as discussed in Ref. [8], and the partitioning of heat supplied to the interface between $q_{c,u}$ and $q_{r,s}$. From a fundamental physics point of view, the transparent interface limit ($f_s = 0$) is closer to the correct description than the opaque interface limit ($f_s = 1$). By present understanding, interface absorption and emission probably only amount to a few percent at most, depending on radiative conditions (spectral distribution, etc.).

2.7 Inputs and Outputs (Problem Types). Various combinations of specified inputs and solved-for outputs are possible. Specified inputs would typically include e-state conditions (relative humidity (RH) and temperature) and any externally imposed radiant flux or radiation source/sink temperature. Unknowns to be solved for would typically include $\dot{m}''$, T_s, and various heat and mass fluxes. The most common of this type of problem is the one with adiabatic Tu-layer, often referred to as the evaporative cooling problem [2] (the name sweat cooling is also used). The first example considered below, the cloud droplet, is an example of the evaporative cooling type of problem (even though the thermodynamic conditions are such that condensation occurs, rather than evaporation). A notable variation of the evaporative cooling problem is the wet-bulb psychrometer problem, which is the most commonly cited textbook example of air/water heat-mass transfer [2–5,9]. In the wet-bulb psychrometer problem (also considered below), T_s is specified by wet-bulb temperature measurement, while e-state relative humidity RH_e is to be determined. Another common variation is the problem in which T_s is specified as an input and some other variable replaces it as an unknown output. This problem is mathematically simpler (less implicit coupling) but physically less realistic in terms of the type of boundary condition information that is most easily and accurately estimated. In Ref. [2], this type of problem is referred to as the drying problem. An example of this type of problem is considered below in the form of sweat cooling (but with specified T_s) of a heated flat-plate with laminar boundary layer flow. The fourth and final example problem considered below, a steam condenser with an air leak taken from Ref. [3], is similar to the evaporative cooling problem in that T_s is unknown; however, the Tu-layer is not adiabatic so this is yet a fourth type of problem.

3 Results and Discussion

3.1 Ex1 Cloud Droplet With Radiation. The first example problem is a spatially isothermal (T_s), quasi-steady cloud droplet residing near the top of a cloud (Fig. 4), losing heat by radiation to a colder, higher layer (e.g., cold sky or upper cloud layer) at $T_r (< T_s)$, and growing by condensation. The droplet with diameter D is small enough to have negligible inertia; i.e., no slip velocity. This problem is akin to the Stefan/Couette flow problem [2–4] and shares the same solution for g/g* ($= \ln(1 + B)/B$). It is the simplest flow that can be treated by the Spalding model and has a no-blowing solution of $Nu_D = Sh_D = 2$ (pure conduction limit). Because of the quasi-steady assumption, the adiabatic Tu-layer condition holds ($q_{c,s} = -(1 - f_s)q_r$ and T-state identical to u-state). The particular case considered here is one treated in Ref. [8] of a 20-μm diameter cloud droplet growing by condensation in a slightly supersaturated atmosphere ($s = 0.001$) at $T_s = 20\,^\circ$C and $P = 70$ kPa while losing heat radiatively to a remote semi-infinite sink (e.g., upper cloud layer) at $T_r = 0\,^\circ$C. The same properties as in Ref. [8] are used here in the Spalding model (see Table 1). The ideal gas polynomial fit for $C_{p,l}(T_s)$ yields $h_{fg,s} = 2454$ kJ/kg, the same as the steam table value to within four significant figures. Radiation is modeled as gray-body emission/absorption by the droplet into a semi-infinite blackbody at T_r

$$q_r = \varepsilon F_{sr} \sigma (T_s^4 - T_r^4) \tag{24}$$

The view factor to a semi-infinite sink is $F_{sr} = 0.5$. The droplet emissivity/absorptivity is assumed to be $\varepsilon = 0.91$ (this parameter also plays the role of droplet absorption/emission efficiency).

Because the atmosphere in this problem is so close to saturation ($|s| \ll 1$), a linearized (Taylor series) closed-form analytical solution is available [8], which is useful because it removes the enthalpy reference and so is independent thereof. This solution, adapted from Ref. [8] for the opposite sign sense of q_r and inclusion of ε in its definition, is (see Appendix for more details)

Table 1 Thermodynamic and transport properties for Ex1—Ex4

Ex#	ρ, kg/m^3	C_p, kJ/kg K	$k \times 10^2$, W/m K	$\alpha \times 10^5$, m^2/s	$\nu \times 10^5$, m^2/s	$D_{12} \times 10^5$, m^2/s	Pr	Sc	Le
1	0.823	1.000	2.60	3.11	2.16	3.58	0.695	0.603	1.15
2	0.512	1.275	4.54	6.95	5.30	9.40	0.763	0.564	1.35
3	1.193	1.005	2.63	2.20	1.57	2.62	0.716	0.599	1.20
4	0.0788	1.890	2.10	14.1	12.6	24.9	0.890	0.504	1.77

$$\Delta T = \frac{s - \mathcal{Q}_r D\frac{\Psi}{H} - \frac{D_c}{D}}{H + \Psi};\quad K_c = \frac{dD^2}{dt} = \frac{4D\dot{m}''}{\rho_\ell} = \frac{\Gamma\left(s + \mathcal{Q}_r D - \frac{D_c}{D}\right)}{H + \Psi} \tag{25}$$

$$H = \frac{h_{fg,s}}{R_w T^2};\quad \Psi = \frac{kR_w T}{D_{12} h_{fg,s} P_{s,e}} = \frac{1.61 P C_p}{P_{s,e} h_{fg,s} Le};\quad \Gamma = \frac{8k}{\rho_\ell h_{fg,s}};\quad \mathcal{Q}_r = \frac{q_r H}{2k} \tag{26}$$

Here, temperature T means either T_s or T_e, since they have nearly the same value for this solution. Their (small) difference is part of the solution: $\Delta T = T_s - T_e$. Also part of the solution is the evaporation or condensation rate. Here, the customary "D-squared law" droplet evaporation "constant" $K_c = dD^2/dt$ has been used to represent the condensation rate. Mass flux is converted to K_c using the liquid density, ρ_ℓ, taken to be 1000 kg/m^3. The quantity D_c is an effective diameter for the Kelvin effect, which accounts for the effect of surface tension on water vapor partial pressure at the droplet surface P_s. Typically, D_c is of order 10^{-3} μm; thus, the Kelvin term is negligible in this example. The term $P_{s,e}$ means $P_s(T_e)$.

Results for Ex1 are shown in Table 2. The analytic solution, Eq. (25), gives $\Delta T = 0.00878$ K and $K_c = 2.25$ μm^2/s. Using the common Reference-A (mismatched reference enthalpies), the Spalding solution gives $\Delta T = 0.00795$ K and $K_c = 2.54$ μm^2/s. This evaporation constant deviates by 13% from the analytic solution [8] of 2.25 μm^2/s. When Reference-B (matched reference enthalpies) is used, the Spalding solution gives $\Delta T = 0.00879$ K and $K_c = 2.28$ μm^2/s, which compares well with the analytic solution. The evaporation constant 2.28 is within a percent of 2.25. The solution with Ref-C gives results nearly identical to those of Ref-B. One quantity that is slightly different between Ref-B and Ref-C is the value of $j_{i,s}h_{i,s}(1 - (1/Le))$. This energy flux is, by definition, zero for Ref-C. For Ref-B this energy flux is slightly nonzero (−0.063 W/m^2), but still much less in magnitude than $q_{c,s}$ (22.9 W/m^2). On the other hand, for Ref-A, $j_{i,s}h_{i,s}(1 - (1/Le))$ is −10.4 W/m^2, which is approximately a third (in magnitude) of the calculated $q_{c,s}$ (31.1 W/m^2). Because of the mismatched vapor enthalpies in Ref-A, the diffusive energy flux term $j_i h_i(1 - (1/Le))$ is not negligible compared to the Fourier conduction flux, and this is the reason for the reduced accuracy of calculated $q_{c,s}$, ΔT, and K_c values with Ref-A. It is interesting to note that if the energy flux $j_{i,s}h_{i,s}(1 - (1/Le)) = -10.4$ W/m^2 in Ref-A is added to the gas-side conduction of 31.1 W/m^2, the resulting flux 20.8 W/m^2 is much closer to the Ref-B and Ref-C solutions for $q_{c,s}$. Since the flux $j_{i,s}h_{i,s}(1 - (1/Le))$ is the amount of energy neglected in the Spalding approximation of the interface energy balance, Eq. (4), this seems like a rational way to correct the gas-side conductive flux.

Regarding radiation modeling, the calculations confirm that the results for surface temperature and condensation rate are independent of the choice of f_s, as is the sum $q_{c,u} + q_{r,s}$. Using Ref-C gives $q_{c,u} + q_{r,s} = -46.88$ W/m^2. This amount of heat comes from conduction from the interface on the gas side, $q_{c,s} = 22.93$ W/m^2, plus the (negative) latent heat liberated at the interface via condensation, $\dot{m}''h_{fg,s} = -69.81$ W/m^2. For the transparent interface option ($f_s = 0$), the modeling assumption is that 46.88 W/m^2 is conducted from the interface into the Tu-layer (i.e., $q_{c,u} = -46.88$), where it is emitted volumetrically to the surroundings ($q_{r,s} = 0$). For the opposite case, the opaque interface ($f_s = 1$), the modeling assumption is that 46.88 W/m^2 ($= -q_{r,s}$) is emitted from the interface to the surroundings, and that there is no conduction of heat from the interface into the Tu-layer, and no volumetric radiant emission from the Tu-layer. For the other references (A and B), the sum $q_{c,u} + q_{r,s}$ is the same, as is the interpretation of how this 46.88 W/m^2 is split between $q_{c,u}$ and $q_{r,s}$ for $f_s = 0$ and 1, respectively.

As for the importance of radiation, if the effect of radiation were made negligible by setting T_r equal to T_e, the condensation constant K_c would drop by over a factor of 2 to 1.07 μm^2/s. That is, radiation to a cold, upper atmosphere layer at 0 °C more than doubles the growth rate of a cloud droplet at the top of a cloud with 0.1% supersaturated air [8]. This problem is a good example of a situation where radiation is likely to be neglected, but is not negligible. Rather, radiation is equivalent to a tenth of a percent change in supersaturation in terms of droplet growth rate. In cloud microphysics modeling, a tenth of a percent is generally considered to be a significant change in supersaturation. In fact, radiative cooling could be an important mechanism in solving the so-called "condensation-coagulation bottleneck", which has puzzled atmospheric scientists for decades, as to how precipitation forms in "warm" (above freezing) clouds, when condensation (without radiation) effectively stops growing droplets at a diameter around 20 μm but coagulation or agglomeration doesn't start growing droplets until a diameter 80 μm (depending on turbulence intensity) [8].

Table 2 Results for Ex1 cloud droplet condensation with radiation

Ex1	A	B	C	Eq. (25)
ΔT, K	0.00795	0.00879	0.00879	0.00878
K_c, μm^2/s	2.54	2.28	2.28	2.25
$q_{c,s}$, W/m^2	31.12	22.98	22.93	22.83
$j_{i,s}h_{i,s}(1 - (1/Le))$, W/m^2	−10.37	−0.063	0	—
$q_{c,s} + j_{i,s}h_{i,s}(1 - (1/Le))$, W/m^2	20.75	22.92	22.93	—

3.2 Ex2 Sweat Cooling of Isothermal Flat Plate Heated Radiatively and Conductively by Forced Convection (Laminar Boundary Layer).

The second example is a flat plate exposed to simultaneous radiative heating and forced convective heating by uniform, parallel flow of hot air (Fig. 5). Cooling of the plate is accomplished by injection of water onto its surface (evaporative cooling) so as to maintain a uniform surface temperature (an inverse square root of x variation in mass and heat fluxes, as shown in Fig. 5, allows this condition). This is an example of a problem with a physical T-state (the temperature of the injected water) but the Tu-layer is not adiabatic. Flow conditions are such that the boundary layer in the gas phase remains laminar over the length of the wetted plate surface. The local [mass, heat] solutions for a laminar, flat-plate boundary layer with mass injection or suction (evaporation or condensation) in the dilute (no-blowing) limit are

$$[Sh_L, Nu_L] = 0.332 Re_L^{1/2} [Sc^{1/3}, Pr^{1/3}] \tag{27}$$

Numerical solutions for g/g* are presented graphically in Refs. [2,3]. An asymptotic solution for "high" B values, less than 1.0 (if $B > 0$) and greater than −0.5 (if $B < 0$), for moderate Pr and Sc values was given in Ref. [1]

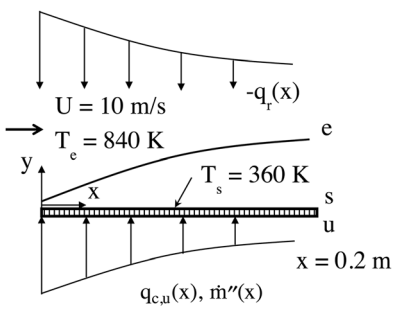

Fig. 5 Schematic diagram of Ex2: sweat cooling of radiatively and convectively heated flat plate with laminar boundary layer

$$\left(\frac{g}{g^*}\right)_{m,h} = \frac{1}{1+0.566B_{m,h}} \left[\text{laminar boundary layer}, -0.5 < B < 1.0\right] \tag{28}$$

Another reasonably accurate curve-fit for moderate [Sc, Pr] values is

$$\left(\frac{g}{g^*}\right)_{m,h} = \frac{1}{(1+B_{m,h})^{0.7}} \left[\text{laminar boundary layer, Sc, Pr} \sim O(1)\right] \tag{29}$$

Note that none of the blowing factor approximations given above, including Couette, have explicitly accounted for Sc or Pr, other than assuming "moderate" values (~1), whereas the exact laminar boundary layer solution does exhibit dependence on Sc and Pr.

The specific case considered here corresponds to Ex. 2.12 and Ex. 2.13 of Ref. [3] called sweat cooling of a flat plate. Dry ambient air at 840 K and 1 atm flows at 10 m/s. The plate surface is maintained at 360 K by injecting water at 300 K (T-state) and allowing it to evaporate. Local conditions are calculated at a point 0.2 m from the leading edge. The same properties (1/2 rule) as in Ref. [3] are used here in the Spalding model (Table 1). The ideal-gas polynomial fit for $C_{p,1}(T)$ yields $h_{fg,s} = 2299$ kJ/kg, slightly greater than the steam table value of 2291 kJ/kg. Because of the relatively high surface temperature in this case, the surface water-vapor mass fraction is much higher than in the previous dilute case of Ex1. As a result, this situation is nondilute in water vapor, and falls in the high mass transfer-rate regime (non-negligible blowing effect: $g/g^* \neq 1$).

Since T_s is prescribed in this problem (drying problem), the mass transfer part of the solution (evaporation rate) does not depend on the choice of enthalpy reference: $m_{1,s} = 0.496$, $B_m = 0.984$, $\dot{m}'' = 7.18 \times 10^{-3}$ kg/m^2 s, with $g_m/g_m^* = 0.57$ taken from the exact laminar boundary layer solution, Fig. 2.30 of Ref. [3]. Note that the Couette blowing factor approximation $\ln(1+B_m)/B_m = 0.70$ would be too high by 23%. The approximation of Eq. (29), $(1+B_m)^{-0.7} = 0.62$, would be noticeably better, within 9%.

The heat transfer part of the solution (see Table 3) does depend on the reference choice. The solution to this problem presented in Ref. [3] uses the Ref-C system, which yields for the net radiant flux $q_r = -15.5$ kW/m^2 and for the gas-side conductive/convective heat flux $q_{c,s} = -2757$ W/m^2. If approximations used in Ref. [3] are relaxed, $q_{c,s}$ changes slightly to -2749 W/m^2 with the Spalding model and Ref-C. Reference-A yields $q_r = -13.2$ kW/m^2. This radiant flux magnitude is 15% lower than that with Ref-C. Reference-B gives $q_r = -15.5$ kW/m^2, which is the same as the reported result for Ref-C. That Ref-B and Ref-C show equivalent results is to be expected since they both match enthalpies between air and water vapor in a similar way; they just do it at different reference temperatures (water triple point versus T_s) and with different reference vapor enthalpies (2501 kJ/kg versus zero). As for the gas-side conducted heat, Ref-B gives $q_{c,s} = -2818$ W/m^2, which is only 2% different from the Ref-C result of $q_{c,s} = -2757$ (or 2749) W/m^2, whereas Ref-A gives $q_{c,s} = -5121$ W/m^2. The energy flux $j_{i,s}h_{i,s}(1-(1/Le))$ is 2433, 71, and 0 W/m^2 for Ref-A,B,C, respectively. The ratio of species diffusive enthalpy flux to Fourier conductive flux magnitude is 48%, 1%, and 0, respectively, for Ref-A,B,C, which explains the loss of accuracy of Ref-A relative to Ref-B and Ref-C. It is again interesting to note that if the energy flux $j_{i,s}h_{i,s}(1-(1/Le)) = 2433$ W/m^2 in Ref-A is shifted from gas-side conduction to liquid-phase radiation absorption, the latter fluxes come much closer to the Ref-B and Ref-C solutions. Specifically, gas conduction $q_{c,s}$ would become $-5121+2433 = -2688$ W/m^2 and q_r would become $-13.2-2.4 = -15.6$ kW/m^2. A flux of 2433 W/m^2 is the amount of energy neglected in the Spalding approximation of the interface energy balance, Eq. (4), with Ref-A. This fact suggests a possible way to correct inaccurate model predictions that have been calculated using mismatched enthalpy references.

Table 3 Results for Ex2 sweat cooling of radiatively and convectively heated flat plate with laminar boundary layer

Ex2	A	B	C	Ref. [3]
q_r, kW/m^2	−13.2	−15.5	−15.5	−15.5
$q_{c,s}$, W/m^2	−5121	−2818	−2749	−2757
$j_{i,s}h_{i,s}(1-(1/Le))$, W/m^2	2433	71	0	—
$q_r - j_{i,s}h_{i,s}(1-(1/Le))$, kW/m^2	−15.6	−15.5	−15.5	—
$q_{c,s} + j_{i,s}h_{i,s}(1-(1/Le))$, W/m^2	−2688	−2747	−2749	—

The same findings about radiation modeling are found again with the flat plate sweat cooling problem as for the droplet problem. The only quantity that depends on the choice of f_s is the fractional split of the sum of $q_{c,s} + \dot{m}''h_{fg,s}$ between $q_{c,u}$ and $q_{r,s}$. Using numbers from the Ref-B solution: $q_{c,s} + \dot{m}''h_{fg,s} = -2818 + 16{,}512 = 13{,}694$ W/m^2. For the transparent interface ($f_s = 0$), the entire 13,694 W/m^2 ($=q_{c,u}$) is conducted to the interface from the Tu-layer, where it was produced by the volumetric absorption of 15,504 W/m^2 of radiant energy minus 1810 W/m^2 that was used to preheat the injected water from 300 K to 360 K. For the opaque interface ($f_s = 0$), 15,504 W/m^2 is absorbed at the interface and 1810 W/m^2 is conducted from the interface into the Tu-layer to preheat the water.

Although the laminar boundary layer has exact, albeit numerical, solutions available for g/g*, approximations for the blowing effect are sometimes used or recommended for this flow. These approximations can become significantly, and needlessly, less accurate in the high mass transfer regime. One example is the stagnant-film (Couette) formula, $\ln(1+B)/B$. Bird et al. [9] pointed out in 1960 (see Ex. 21.7-1 of Ref. [9]) that the stagnant-film approximation incurs increasing inaccuracy for nondilute laminar flat-plate flow. Yet it is still often used and cited in textbooks, for example, as recently as 2015 in Ex. 11.16 of Ref. [4]. If analytic approximations are desired for g/g*, Eqs. (21) and (22) are better in terms of accuracy than the stagnant film (Couette flow) approximation. In the present sweat cooling example, the exact solution for heat transfer blowing factor is $g_h/g_h^* = 0.52$. The Couette flow approximation, $\ln(1+B_h)/B_h = 0.64$, is too high by 23%. On the other hand, the formula $(1+B_h)^{-0.7} = 0.56$ is within 7% of the exact blowing factor.

Note that although this problem is posed as a Drying problem (prescribed $T_s = 360$ K) with $q_r = -15.5$ kW/m^2 being solved for, the more natural boundary condition in practice would be for $q_r = -15.5$ kW/m^2 to be prescribed and T_s to be solved for, i.e., evaporative cooling problem.

3.3 Ex3 Wet-Bulb Psychrometer With and Without Radiation.

The third example problem is the classic wet-bulb psychrometer problem. This is the most popular textbook example of water/air heat and mass transfer [2–5,9]. The wet-bulb psychrometer is a thermometer or thermocouple wrapped in a water-soaked fabric or wetted wick (Fig. 6). It is cooled by evaporative cooling and in its intended mode of operation is at quasi-steady state. Fluid dynamically the wet-bulb psychrometer can be modeled as a cylinder of diameter D in moist air moving with Reynolds number Re_D (Fig. 6). Due to the complexity of the flow around the cylinder, there is no exact solution for integrated Nu_D, Sh_D, or g/g* around the circumference of the cylinder. However, empirical correlations for Nu_D and Sh_D have been developed that can be used with good confidence for this problem. The following simple correlation is often used:

$$[Sh_D, Nu_D] = CRe_D^{1/2}[Sc, Pr]^{1/3} \tag{30}$$

Sometimes the 1/3 exponent on [Sc,Pr] is replaced with a different power, such as 0.4. A slightly more complicated relation that

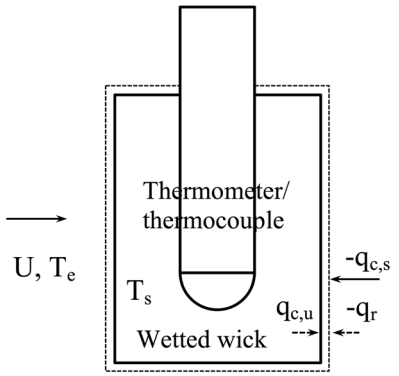

Fig. 6 Schematic diagram of Ex3: wet-bulb psychrometer with and without radiation

effectively modifies the 1/3 exponent on [Sc,Pr] is the Churchill and Bernstein correlation from Ref. [10]

$$[Sh_D, Nu_D] = 0.3 + \frac{0.62 Re_D^{1/2}[Sc,Pr]^{1/3}}{\left[1 + 0.4/[Sc,Pr]^{2/3}\right]^{1/4}}, \quad Re_D < 10^4 \quad (31)$$

More sophisticated correlations, which are routinely available in texts, are not justified in the wet-bulb psychrometer problem because, as explained below, the operation of the device and the desired output (ambient relative humidity) are only weakly dependent on the flow conditions.

The blowing parameter g/g* has not been well characterized for cylinder flow. Fortunately, psychrometric applications are usually in the dilute limit and the choice of g/g* ($\sim$1) is not very important ($\ln(1+B)/B$ is satisfactory).

The adiabatic Tu-layer condition applies to the wet-bulb thermometer ($q_{c,s} = -(1-f_s)q_r$ and T-state identical to u-state) and thus B_h can be written as

$$B_h = \frac{h_e - h_s}{h_s - \left(h_u - \dfrac{q_r}{\dot{m}''}\right)} = \frac{h_e - h_s}{h_s - \left(h_u - \dfrac{q_{c,u}}{\dot{m}''}\right)}, \quad [\text{adiabatic Tu} - \text{layer}] \quad (32)$$

The desired operating condition for a psychrometer is to have the evaporation rate be high enough that the terms involving heat flux-to-mass flux ratio in the denominators of Eq. (32) are negligible compared with $(h_s - h_u)$. The magnitude of $(h_s - h_u)$ depends on the enthalpy reference choice. Reference-C gives: $(h_s - h_u) = h_{fg,s}$. Reference-B gives nearly the same result: $(h_s - h_u) = h_{fg,0} - (C - C_{p2})T_s(°C) = h_{fg,s} - (C_{p1} - C_{p2})T_s(°C)$, which is very nearly (slightly less than) $h_{fg,s}$. For this condition, B_h becomes

$$B_h = \frac{h_e - h_s}{h_s - h_u}, \quad \left|\frac{q_r}{\dot{m}''}\right| \ll (h_s - h_u) = h_{gf,s} \; [\text{psychrometer, Ref} - C] \quad (33)$$

In the dilute limit, when enthalpy-matched Ref-C is used (and even when Ref-B is used), the vapor mixture enthalpies $h_{e,s}$ can be approximated as the enthalpies of just species-2 (air) such that their difference $h_e - h_s$ becomes $C_{p2}(T_e - T_s)$

$$B_h = \frac{C_{p2}(T_e - T_s)}{h_{fg,s}}, \quad \left|\frac{q_r}{\dot{m}''}\right| \ll h_{fg,s} \; [\text{psychrometer, Ref} - C] \quad (34)$$

Further implementation of the psychrometer conditions (e.g., $B_m = m_{1,s} - m_{1,e}$, $g_h/g_m = (g_h/g_m)^* = Le^{-2/3}$) in $B_m = (g_h/g_m)B_h$ leads to the well-known, simple, closed-form expression for the e-state water vapor mass fraction [2–4]

$$m_{1,s} - m_{1,e} = Le^{-2/3}\frac{C_{p2}}{h_{fg,s}}(T_e - T_s), \quad \left|\frac{q_r}{\dot{m}''}\right| \ll h_{fg,s} \; [\text{psychrometer, Ref-C}] \quad (35)$$

where the simple correlation for [Sh,Nu] with 1/3 power on [Sc,Pr] has been used to determine the Le exponent of $-2/3$.

The particular conditions considered first are those presented in Ref. [2] of a wet-bulb reading of $T_s = 16\,°C$ and a dry bulb reading of $T_e = 27\,°C$ at 101.3 kPa with a negligible radiant flux effect. Properties are listed in Table 1 (Ex3). For these conditions, $m_{1,s} = 0.0112$, $C_{p2} = 1.005$ kJ/kg K, $h_{fg,s} = 2464$ kJ/kg K, and Le = 1.195 (the same Lewis number as in Ref. [2]). The closed-form analytic solution, Eq. (35), gives $m_{1,e} = 0.00722$ ($RH_e = 0.329$). The Spalding model with Ref-C gives $m_{1,e} = 0.00726$ ($RH_e = 0.329$). The Spalding model with Ref-A and Ref-B gives $m_{1,e} = 0.00680$ ($RH_e = 0.309$) and $m_{1,e} = 0.00725$ ($RH_e = 0.329$), respectively (Table 4). Clearly, the choice of enthalpy reference state makes a difference with enthalpy-matched references Ref-C and Ref-B being preferable over Ref-A. As in the previous example, this trend can be explained by the ratio of species diffusive enthalpy flux to Fourier conductive flux magnitude, which is 16%, 0.09%, and 0, respectively, for Ref-A,B,C. Again adding the energy flux $j_{i,s}h_{i,s}(1 - (1/Le))$ to the gas-side conduction $q_{c,s}$ helps correct the error in the latter flux, especially for Ref-A.

The solution to this example problem as presented in Ref. [2] includes several errors and sources of inaccuracy of varying degree that need comment. First, a minor error in Eq. (20-18) of Ref. [2] is the unnecessary replacement of $h_{fg,s}$ with $h_{fg,0}$. It is true that the two values are within a few percent typically but since T_s is known in this problem type, the more accurate $h_{fg,s}$ is as easy to evaluate as the less accurate $h_{fg,0}$. Second, another minor point, is that in Eq. (20-20), the justifying equation cited, Eq. (10-22), is a local result for the stagnation line of a cylinder, but what is needed is the integrated result around the circumference of the cylinder, something more like Eq. (10-55), or the simple correlation for [Sh,Nu] with 1/3 power on [Sc,Pr], or even the Churchill and Bernstein correlation. An algebraic error also occurs in Eq. (20-20), where the exponent on Le (=Pr/Sc) is incorrectly put as 0.4 instead of $(0.4 - 1) = -0.6$. Next, a significant error occurs in the numerical evaluation of relative humidity when the saturation pressure based on T_s is used rather than that based on T_e, resulting in an erroneously high value of $RH_e = 0.55$. Finally, the idea that using Le = 1 introduces only a slight error is discussed in Ref. [2]. The enthalpies used in that evaluation follow Ref-A, which introduces its own source of error as noted above. Thus, the error due to using Ref-A and that due to using Le = 1 are confounded. Using the Spalding solution to isolate these errors shows that each assumption (Le = 1 and Ref-A) introduces about the same amount of error in the wet-bulb psychrometer evaluation of RH_e.

Next, the effect of radiant flux, which has been neglected in the preceding calculations, is included. Radiation from the ambient e-state to the wet-bulb s-state can make a measureable difference in wet-bulb psychrometer results. The closed-form solution, Eq. (35), cannot estimate the radiation effect, but the full Spalding solution can. A wet-bulb psychrometer would normally be subject to blackbody radiation from isothermal surroundings at T_e. The

Table 4 Results for Ex3 wet-bulb psychrometer without radiation

Ex3 $q_r = 0$	A	B	C	Eq. (35)
$m_{1,e}$	0.00680	0.00725	0.007255	0.00722
RH_e	0.309	0.329	0.329	0.329
$q_{c,s}$, W/m^2	−10,281	−9235	−9230	—
$j_{i,s}h_{i,s}(1 - (1/Le))$, W/m^2	1696	8.3	0	—
$q_{c,s} + j_{i,s}h_{i,s}(1 - (1/Le))$, W/m^2	−8585	−9227	−9230	—

wet-bulb thermometer can be modeled as a cylindrical graybody with the emissivity of water. Thus, Eq. (24) can be used for estimating radiation with the r-state of Eq. (24) replaced by the e-state: $T_r \rightarrow T_e$ and $F_{sr} \rightarrow F_{se} = 1$. A cylinder diameter of $D = 1.5$ mm and emissivity of 0.96 are assumed here, giving $q_{c,u} = -(1 - f_s)q_r = 61.2\ W/m^2$.

With radiation included in the analysis, the inferred e-state humidity depends on mass transfer rate, and thus on the speed of the airflow over the wet-bulb thermometer. Using either Ref-C or Ref-B in the Spalding model with air speeds of $U = 0.3$, 3, and 30 m/s and the Churchill/Bernstein correlation results in $m_{1,e} = 0.00685$ ($RH_e = 0.311$), $m_{1,e} = 0.00712$ ($RH_e = 0.323$), and $m_{1,e} = 0.00721$ ($RH_e = 0.327$), respectively, as shown in Table 5. Clearly, the higher the air speed (higher evaporation rate), the closer the solution is to the no-radiation solution presented in Table 4. To approach the no-radiation solution within three significant figures would require an unrealistically high air speed (>100 m/s). Thus, wet-bulb humidity measurements are unavoidably influenced by radiation effects that are possibly built into psychrometric charts based on experimental data. In this example, a psychrometric chart reading of $RH_e = 0.31$ [7] could be indicative of the effects of radiation and finite mass transfer rate with air speed of approximately $U = 0.3$ m/s over a 1.5-mm diameter wet-bulb thermometer.

This example of the wet-bulb psychrometer illustrates that (i) the use of an ill-chosen enthalpy reference can lead to inaccurate results, (ii) radiation can have a significant influence on inferred results, even at room temperature conditions, and (iii) setting $Le = 1$ is not a necessary or useful approximation when obtaining numerical results; more accurate results are obtained with the actual Le.

3.4 Ex4 Effect of Air Leak on Condenser Performance.

The fourth and final example problem, taken from Ref. [3], illustrates the effect of a small amount of air on heat transfer and condensation rates in a tube-in-shell steam condenser (Fig. 7). As in the previous example, crossflow over a cylinder defines the fluid mechanics. Unlike in the previous example, this problem is not dilute in water vapor and not diffusion-dominated, low-rate mass transfer. In fact, it is the opposite limit. The vapor mixture in the e-state is dilute in air and the problem is one of high-rate mass transfer. The choice of a blowing factor model—again, not well-characterized for cylinder crossflow—is nevertheless very important. Another unique aspect of this problem, different from all the previous ones, is that there is a significant heat flux that is conducted into the condensing liquid water, $-q_{c,u}$, (primarily the latent heat from condensing steam, $\dot{m}''h_{fg,s}$), which is then conducted through the tube wall and into cooling water flowing inside tubes. Thus, there is no physical T-state. The details of this problem, taken from Ex. 2.9 [3], are as follows.

Table 5 Results for Ex3 wet-bulb psychrometer with radiation (Ref-C)

Ex3 $q_r = -61\ W/m^2$; U	0.3 m/s	3 m/s	30 m/s	100 m/s
$m_{1,e}$	0.00685	0.00712	0.00721	0.00723
RH_e	0.311	0.323	0.327	0.328
$q_{c,s}$, W/m^2	−560	−1646	−5081	−9230

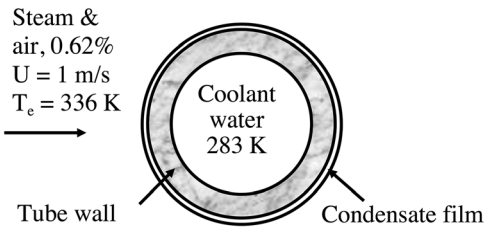

Fig. 7 Schematic diagram of Ex4: effect of air leak on condenser performance

Steam at $T_e = 336$ K and $P = 0.115$ atm (11.65 kPa) containing 0.62% air by mass ($m_{1,e} = 1 - 0.0062 = 0.9938$) flows at 1 m/s over a horizontal brass condenser tube of 19.1 mm O.D. and 16.1 mm I.D., as shown in Fig. 7. Coolant water flows through the tube at a bulk velocity of 1.47 m/s. The unknowns to be found are the steam condensation rate and other associated unknowns at an axial tube location where the bulk coolant temperature is $T_c = 283$ K. Other associated unknowns include the vapor/condensate interface temperature, T_s, the condensate-tube outer wall interface temperature T_{ow}, the coolant-tube inner wall temperature T_{iw} (if desired), and the effective thickness of the condensate layer (see wall detail schematic diagram, Fig. 8). Assumptions to be made are that the thickness of the condensate film is negligible in estimating g* and that the tube is isothermal circumferentially. The same properties as in Ref. [3] are used (Table 1), which are those for pure steam at an estimated film temperature of 320 K.

One slight calculation difference between [3] and the Spalding model is that [3] assumes $q_{c,s}$ is negligible and uses the species-grouping interface energy equation, whereas the Spalding model includes $q_{c,s}$ implicitly in the molecular heat flux. As shown in Ref. [3], and as can be shown by the Spalding model solution, $q_{c,s}$ is indeed negligible compared with the latent heat flux, $\dot{m}''h_{fg,s}$.

In lieu of a T-state, additional equations are needed to describe the region between the u-surface (T_s) and the coolant (T_c). There are three elements in series that each contribute a heat transfer resistance (Fig. 8): the condensate layer on the outside of the tube (T_s to T_{ow}), the tube wall (T_{ow} to T_{iw}), and the liquid water boundary layer inside the tube (T_{iw} to T_c). Using standard expressions [4,10] for laminar film condensation and internal turbulent flow in a tube with appropriate properties inserted, the following equations are obtained:

$$-q_{c,u} = \frac{\dot{Q}}{A_o} = h_o(T_s - T_{ow}) \tag{36}$$

$$h_o = 0.728\left[\frac{(\rho_\ell - \rho)g h_{fg,s} k_\ell^3}{\nu_\ell D(T_s - T_{ow})}\right]^{1/4} = 17{,}300(T_s - T_{ow})^{-1/4}$$
$$= \frac{10^5}{5.78}(T_s - T_{ow})^{-1/4} \tag{37}$$

The equations above describe the first of the three elements: laminar film condensation on the outside of the tube with area A_o. The units of heat transfer coefficient h_o are W/m^2 K. The next equations are similar but for the combined three elements in series and the overall heat transfer coefficient U_o in W/m^2 K. The constant 22.6 accounts for the combined tube conductive and turbulent convective resistances

$$-q_{c,u} = \frac{\dot{Q}}{A_o} = U_o(T_s - T_c) \tag{38}$$

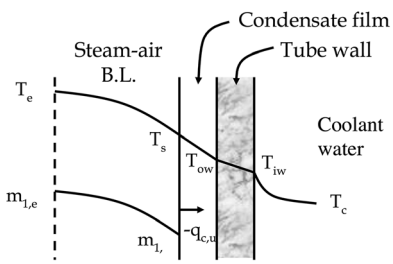

Fig. 8 Schematic diagram of Ex4: detail of tube wall

$$\frac{1}{U_o A_o} = \frac{1}{A_o}\left[\frac{10^5}{22.6 + 5.78(T_s - T_{ow})^{1/4}}\right]^{-1} \tag{39}$$

Combining the above equations to eliminate $(T_s - T_{ow})$ gives the necessary equation to add to the Spalding equations to solve the problem

$$-q_{c,u} = \frac{(T_s - 283\text{K})10^5}{22.6 + 5.78\left(\frac{-q_{c,u}}{17{,}300}\right)^{1/3}} \tag{40}$$

In Ref. [3], the Couette flow (stagnant film) blowing factor $\ln(1+B)/B$ was used to solve the problem. Using that same blowing factor, the Spalding model gives results shown in Table 6. All three references, A, B, and C, give similar results for T_s (304 K), heat flux to the tubes, $-q_{c,u}$ (67 kW/m^2), and condensation rate (0.027 kg/m^2 s). Even Ref-A, which gave aberrant results in previous examples, gives results similar to those of Ref-B and Ref-C in these quantities. This is because the magnitude of $-q_{c,u}$ is so large in this problem that the flux $j_{i,s}h_{i,s}(1-(1/Le))$ is small compared to fluxes like $q_{c,s}$, even for Ref-A. Still, the deduced gas conductive heat flux $q_{c,s}$ magnitude for Ref-A (50 kW/m^2) compared with the other solutions (2 kW/m^2) is too high by over an order of magnitude.

While the Couette flow blowing factor is often a suitable choice when no better information is available, this example is one case where it should be questioned. This is because this problem is in the high (negative) mass transfer rate limit ($B \sim -1$). A logical alternative blowing factor is the laminar boundary layer blowing factor. This is because for the Reynolds number of this cylinder flow ($Re_D = 152$), a significant part of the flow over the tube is occupied by laminar boundary layer. The Spalding model solutions with the approximation $g/g^* = (1+B)^{-0.7}$ are shown in Table 7. Again, there is little change in the quantities T_s (320 K), heat flux to the tubes, $-q_{c,u}$ (111 kW/m^2), and condensation rate (0.046 kg/m^2 s) between the three references, but the differences in these quantities between the laminar boundary layer blowing factor (Table 7) and the Couette flow blowing factor (Table 6) are quite noticeable. Results between these two blowing factors (using the more accurate Ref-B,C) are compared in Table 8, along with the solution for pure steam (no air leak). The Couette flow blowing factor gives a condensation rate that is only 56% of that for the pure steam case and a heat flux to the tubes ($-q_{c,u}$) that is only 57% of that for pure steam. This seems like a rather large reduction or penalty in performance, given that air comprises only 0.62% of the bulk steam mixture, as noted in Ref. [3]. The laminar boundary layer blowing factor gives a condensation rate that is 96% of that for the pure steam case and a heat flux to the tubes ($-q_{c,u}$) that is 95% of that for pure steam. This seems like a more reasonable performance penalty, given the small amount of air leak. However, it is not possible to say how accurate even this prediction is, without more sophisticated analysis of the entire flow regime, including the turbulent wake region. What can be concluded about the air leak problem is that a small amount of noncondensable gas (air) leaking into a steam condenser has a disproportionate penalty effect on performance, because it tends to accumulate near the tube surface where it impedes the transport of steam to the tubes, but the amount of the penalty according to the Spalding model could vary from a few percent to a few tens of percent, depending on the effective blowing factor. Whether the air accumulation at the tube surface is as much as that predicted by the Couette flow blowing factor ($m_{1s} = 0.28$) seems questionable.

Table 6 Results for Ex4 effect of air leak on condenser with Couette flow (stagnant film) blowing factor

Ex4 Couette flow	A	B	C	Ref. [3]
T_s, K	304	304	304	304
$q_{c,u}$, W/m^2	−66,612	−66,921	−66,899	−65,500
$\dot{m}''$, kg/m^2 s	−0.0269	−0.0269	−0.0269	−0.0270
$q_{c,s}$, W/m^2	−50,015	−2110	−1599	−1650
$j_{i,s}h_{i,s}(1-(1/Le))$, W/m^2	−21.18	−0.22	0	—

Table 7 Results for Ex4 effect of air leak on condenser with laminar boundary layer blowing factor

Ex4 laminar B.L.	A	B	C
T_s, K	320	320	320
$q_{c,u}$, W/m^2	−111,076	−111,093	−111,087
$\dot{m}''$, kg/m^2 s	−0.0460	−0.0459	−0.0459
$q_{c,s}$, W/m^2	−16,563	−1649	−1411
$j_{i,s}h_{i,s}(1-(1/Le))$, W/m^2	−6.7	−0.106	0

Table 8 Effect of blowing factor in Ex4: Couette flow (stagnant film) versus laminar boundary layer

	0.62% air, blowing factor		
Ex4	Couette flow (stagnant film)	Laminar B.L.	Pure steam
T_s, K	304	320	322
$m_{1,s}$	0.284	0.868	1
B_m	−0.991	−0.953	−1
g_m/g_m^*	4.8	8.5	$\rightarrow\infty$
$\dot{m}''$, kg/m^2 s	−0.0269	−0.0459	−0.0480
$q_{c,u}$, W/m^2	−66,900	−111,000	−116,380
$q_{c,u}$ ratio	0.57	0.95	1
Percentage reduction	43%	5%	—

The laminar boundary layer blowing factor gives a condensation rate that is 96% of that for the pure steam case and a heat flux to the tubes ($-q_{c,u}$) that is 95% of that for pure steam. This seems like a more reasonable performance penalty, given the small amount of air leak. However, it is not possible to say how accurate even this prediction is, without more sophisticated analysis of the entire flow regime, including the turbulent wake region. What can be concluded about the air leak problem is that a small amount of noncondensable gas (air) leaking into a steam condenser has a disproportionate penalty effect on performance, because it tends to accumulate near the tube surface where it impedes the transport of steam to the tubes, but the amount of the penalty according to the Spalding model could vary from a few percent to a few tens of percent, depending on the effective blowing factor. Whether the air accumulation at the tube surface is as much as that predicted by the Couette flow blowing factor ($m_{1s} = 0.28$) seems questionable.

Another interesting result that comes out of the air leak example is the magnitude of the condensate film thickness. This can be estimated as the ratio of the condensate thermal conductivity k_ℓ to h_o. For the laminar boundary layer case, this ratio (0.64 W/m K)/(9310 W/m^2 K) is 69 μm, supporting the assumption of neglecting the film thickness relative to tube diameter in calculating g*.

The effect of radiation has been neglected in the air leak example. This assumption can be confirmed by including radiation in the calculation. To include radiation, one possible limiting assumption that can be made about the radiation environment is that the tube is surrounded by a blackbody at T_e. This situation would arise if the tube were part of an array of tubes with the steam between tubes being optically thick. Another possible limiting assumption about the radiation environment is that the tube is surrounded by a blackbody at T_s. This situation would arise if the tube were part of an array of identical tubes with the steam being optically thin. In either limiting case, the radiation effect is negligible.

4 Conclusions

Several simple ways of improving the accuracy of the Spalding model results for air/water evaporation/condensation problems are pointed out. First is the choice of thermodynamic reference state for enthalpy evaluation. The theoretical formulation of the Spalding model and comparison of its predictions with analytic solutions suggests that choosing the interface temperature as reference point and setting both air and water-vapor enthalpies at that point to the same numerical value gives the most accurate results. This approach was illustrated with Ref-C, where zero was chosen as the gas-phase reference enthalpy. Choosing 0 °C as the reference point and again setting both air and water-vapor enthalpies at that point to the same value gives almost identical results to the first option. This second approach was illustrated with Ref-B, where

$h_{fg,0} = 2501$ kJ/kg was selected as the gas-phase reference enthalpy. The common practice of choosing the steam table reference point (0.01 °C) with water-vapor enthalpy of $h_{fg,0}$ and air enthalpy of zero introduces an unnecessary enthalpy mismatch between air and water vapor that compromises accuracy of results, particularly the gas-side conductive heat flux $q_{c,s}$. This flux can be partially corrected by adding to it the neglected partial species diffusion flux, $j_{i,s}h_{i,s}(1 - (1/Le))$, which was neglected in the similarity solution. Still, this kind of correction is not necessary if Ref-B or Ref-C is adopted in the first place. While Ref-C might seem like the best possible solution because it sets $j_{i,s}h_{i,s} = 0$ identically, we must keep in mind that this condition can be forced to happen at only one thermodynamic state, in this case at the interface. There are still other y-locations in the gas-phase where the flux j_ih_i is not identically zero, and an approximation is still being made in the similarity solution in neglecting $j_ih_i(1 - (1/Le))$ in the molecular flux. The small error involved in using Ref-C has not been evaluated here.

Another simple way of improving the accuracy is the judicious choice of blowing factor in high-rate mass transfer situations. For example, the laminar boundary layer blowing factor may be significantly more accurate than the common stagnant-film (Couette flow) blowing factor for flat plate flow and even cylinder crossflow, under laminar flow conditions. The importance of blowing factor in high transfer-rate condensation with laminar cylinder crossflow was illustrated by the steam condenser example in evaluating the effect of a small air leak on condenser performance.

Radiation often makes an important contribution in air/water heat and mass transfer problems that can usually be included without sophisticated radiative transfer modeling. Two common but opposite assumptions about radiation participation in water, transparent interface and opaque interface, are shown to be equivalent for most purposes. The only difference comes in the temperature profile in the liquid water near the interface and the partitioning of energy flow between surface absorption/emission and conduction in the liquid near the interface. A methodology is introduced for modeling true interfacial absorption/emission associated with phase change if/when the amount of this effect becomes known well enough to justify its inclusion. In the mean time, either the transparent interface or opaque interface assumption works equally well for infrared radiation, although the former is probably physically more correct, as phase-change interfacial absorption/emission probably only amounts to 3–6% effect. The importance of including radiation was illustrated in several examples, including cloud droplet condensation, sweat cooling, and the wet-bulb psychrometer.

Finally, while the error introduced by setting $Le = 1$ may be no larger than error and uncertainty introduced by other sources, such as input parameter uncertainty, there is no reason to unnecessarily introduce the error associated with using $Le = 1$ in the air/water Spalding model when $Le \neq 1$ can just as easily be evaluated.

Acknowledgment

The support of the Hermia G. Soo Professorship and NSF Grant No. 1457128 helped make this research possible.

Nomenclature

A_o = outer area of tube
$B_{m,h}$ = Spalding B-number for mass or heat transfer
C = liquid water specific heat, 4.2 kJ/kg K
C_p = vapor specific heat
D = diameter of droplet, cylinder, etc.
D_{12} = binary diffusion coefficient of water (1) in air (2)
f_s = interfacial radiation parameter combining $f_{s,ab}$ and $f_{s,em}$
$f_{s,ab}$ = fraction of radiation absorbed at interface
$f_{s,em}$ = fraction of radiation emitted at interface
F_{sr} = radiation view factor from surface (s) to radiative environment (r)
$g_{m,h}$ = Spalding gradient term or conductance for mass or heat transfer
h = vapor-phase mixture enthalpy (mass specific), $m_1h_1 + m_2h_2$
h_i = vapor-phase enthalpy (mass specific) for water ($i = 1$) or air ($i = 2$)
h_o = outer convective heat transfer coefficient on tube
h_r = radiative heat transfer coefficient
h_{fg} = latent enthalpy of evaporation for water
j_i = vapor-phase diffusive mass flux for water ($i = 1$) or air ($i = 2$)
k = vapor thermal conductivity
k_ℓ = liquid water thermal conductivity
K_c = droplet condensation rate constant, dD^2/dt
L = characteristic length scale, e.g., diameter D
Le = Lewis number, $D_{12}/\alpha = Pr/Sc$
m_1 = water mass fraction in vapor phase
m_2 = air mass fraction in vapor phase
$\dot{m}''$ = water mass flux at vapor–liquid interface
Nu = Nusselt number
P = total pressure
P_s = water saturation pressure at T_s
$P_{s,e}$ = saturation pressure at T_e
P_1 = water vapor partial pressure
Pr = Prandtl number, ν/α
$q_{r,c,fg}$ = heat flux (r = radiative, c = conductive, fg = latent)
R_w = gas constant for water, 8.314/18 kJ/kg K
Re_L = Reynolds number, UL/ν
RH = relative humidity, $P_1(T)/P_s(T)$
s = supersaturation, $RH_e - 1$
Sc = Schmidt number, ν / D_{12}
Sh = Sherwood number
T = temperature
T_e = environment or e-state temperature
T_r = effective radiation environment temperature
T_s = air–water interface temperature
$\Delta T = T_s - T_e$
u,v = bulk (mass-average) vapor velocity in the x,y-direction
U = characteristic velocity
U_o = overall heat transfer coefficient based on A_o
x = coordinate parallel to the interface
y = coordinate perpendicular to interface, positive into gas phase

Greek Symbols

α = vapor thermal diffusivity
ε = emissivity
ν = vapor momentum diffusivity (kinematic viscosity)
ν_ℓ = water liquid kinematic viscosity
ρ = vapor density
ρ_ℓ = water liquid density
σ = Stefan–Boltzmann constant, 5.67×10^{-8} W/m^2 K^4

Subscripts

ab = absorbed (radiation)
c = conductive/convective, characteristic, or coolant
e = thermodynamic state of vapor environment
em = emitted (radiation)
fg = saturated liquid–vapor phase change
i = species index, 1 (water) or 2 (air)
iw = inner wall
ℓ = liquid water
L = length scale in vapor phase
ow = outer wall
r = radiative
s = thermodynamic state in vapor at liquid–vapor interface

T = thermodynamic state in liquid removed from interface
tp = triple point of water, 0.01 °C, 0.6113 kPa
u = thermodynamic state in liquid at liquid–vapor interface
w = water
1,2 = species: water, air

Superscript

* = low mass-transfer rate or dilute limit

Appendix

Details of the quasi-steady cloud droplet problem and the derivation of Eq. (25) are presented here. Based on optical and other thermophysical properties of water, the droplet is assumed to be spatially isothermal at T_s (see Ref. [8] for further justification of this assumption). The unsteady mass balance on a droplet of radius R (=D/2) is

$$\rho_\ell \frac{dR}{dt} = -\dot{m}'' \tag{A1}$$

and the energy balance (s-surface) is

$$-\rho_\ell C \frac{R}{3}\frac{dT_s}{dt} = q_{c,s} + q_r + \dot{m}'' h_{fg,s} \tag{A2}$$

The conduction term for a cloud droplet with typical size of $R = 10\,\mu$m is in the pure conduction limit, i.e., no convection (no velocity slip), for which $Nu_R = 1$

$$q_{c,s} = \overbrace{Nu_R}^{1}\frac{k}{R}(T_s - T_e) \tag{A3}$$

The characteristic time constant for transient behavior depends on which terms in the energy balance dominate. In most situations the conduction term will be important, whereas the radiation and phase-change terms may or may not be important, depending on conditions. Therefore, the time constant τ can be estimated by taking a balance between the storage and conduction terms. Approximating dT_s/dt as $|T_s - T_e|/\tau$ gives for the time constant

$$\tau = \frac{\rho_\ell C R^2}{3k} \tag{A4}$$

The time constant for a cloud droplet ($R = 10\,\mu$m) would be: $\tau = 5$ ms. Cloud droplets are typically assumed to be quasi-steady over time scales of importance fluid mechanically in cloud dynamics. This is a significant mathematical simplification because the droplet energy equation changes from differential to algebraic. The quasi-steady assumption involves neglecting the storage term (left-hand side) of the droplet energy equation to give, for the s-surface equation

$$0 = q_{c,s} + q_r + \dot{m}'' h_{fg,s} \tag{A5}$$

Equation (A5) can be seen to be equivalent to Eq. (16) when Eq. (18) and the adiabatic Tu-layer condition, $q_{c,u} = -(1 - f_s)q_r$, are applied. It can be shown that Eq. (A5) with Eq. (A3) is equivalent to the equations presented above in terms of B_m and B_h, e.g., Eqs. (6) and (7). If (a) the equations for mass flux involving B_m and B_h (which assume quasi-steady liquid), i.e., Eqs. (6) and (7), are combined, (b) adiabatic liquid is imposed, and (c) vapor enthalpies are evaluated using the dilute (in water vapor) approximation, the same algebraic equation for quasi-steady droplet temperature is obtained

$$\Delta T \equiv T_s - T_e = -\frac{R}{k}\left(q_r + \dot{m}'' h_{fg,s}\right) \tag{A6}$$

where

$$\dot{m}'' = \frac{\rho D_{12}}{R}\ln(1 + B_m) = \frac{\rho D_{12}}{R}(m_{1,s} - m_{1,e}) \quad \text{(dilute in water vapor)} \tag{A7}$$

Equations (A6) and (A7) appear to be explicit in T_s (left-hand side) but are actually implicit because of the right-hand side terms $m_{1,s}(T_s)$ and $q_r(T_s)$. Still they are algebraic and can be solved for T_s without integrating, which is the essential simplification of the quasi-steady droplet assumption. The water vapor mass fractions in Eq. (A7) can be converted to partial pressures, $P_{1,s}$ and $P_{1,e}$, using the ideal gas assumption. The latter can be related to relative humidity (RH) of the ambient environment (e-state). The partial pressures, assuming local thermodynamic equilibrium at the droplet surface, can be taken as the saturation pressure, $P_s(T_s)$, after adjustments for solute and curvature effects, as necessary.

It is common in the literature, particularly on cloud microphysics, to work with a combined droplet energy/mass equation. Combining the algebraic energy equation (A6) with the mass equation (A1) gives

$$R\frac{dR}{dt} = \frac{k}{\rho_\ell h_{fg,s}}\left[\underbrace{T_s - T_e}_{\Delta T} + \frac{q_r R}{k}\right] \tag{A8}$$

For quasi-steady, conduction-dominated ($q_r = 0$) evaporation or condensation, T_s is constant. Therefore, mass flux varies as 1/R (see Eq. (A7)) and dR^2/dt is constant, the so-called D-squared evaporation law

$$T_s = \text{const}; \quad \dot{m}'' = \frac{\text{const}}{R}; \quad \frac{dR^2}{dt} = \frac{-2R\dot{m}''}{\rho_\ell} = \text{const.} (q_r = 0) \tag{A9}$$

Cloud droplets typically exist in a nearly saturated thermodynamic environment. Therefore, the quasi-steady droplet mass and energy equations developed above are specialized to conditions near saturation. Introducing the supersaturation, s, defined as relative humidity minus one: $s = RH - 1$, we can apply the concept of supersaturation to the thermodynamic e-state, which is never far from saturation in a cloud (perfect saturation over a flat interface of pure water means $s = 0$). A typical magnitude of s in stable clouds is less than a fraction of a percent. The largest values occur in developing convective clouds with strong vertical motions. In these clouds, adiabatic cooling induced by updrafts with velocities of the order meters per second can drive s as high as a few percent, but only for a few minutes or tens of minutes. Then s returns to a fraction of a percent as thermodynamic equilibrium is re-established (that s does not go identically to zero is due primarily to the Kelvin effect, which is the surface-tension or droplet curvature effect, and the solute effect). In the core of the cloud, the sign of s is generally positive; on the edges it can fluctuate positive or negative due to mixing with drier surrounding air. But in either case the magnitude is small such that near-saturation conditions prevail: $|s| \ll 1$.

Next, the Clausius–Clapeyron equation is introduced to describe the variation of saturation pressure (equilibrium vapor-pressure over a flat interface) with temperature. In an integrated form (assuming $h_{fg,s}$ constant, which is valid for small deviations from saturation), the Clausius–Clapeyron equation is

$$\frac{P_s(T_s)}{P_s(T_e)} = \exp\left[\frac{h_{fg,s}}{R_w}\left(\frac{1}{T_e} - \frac{1}{T_s}\right)\right] \tag{A10}$$

Furthermore, for small supersaturation values the following approximation can be used:

$$\frac{h_{fg,s}|\Delta T|}{R_w T^2} \ll 1; \quad T_s \approx T_e (= T); \quad \Delta T \equiv T_s - T_e \tag{A11}$$

Here, ΔT is the (small) deviation of the droplet temperature from the environment (air) temperature. It is small because of, or, in the sense that, $|s| \ll 1$. Finally, Taylor series expansions are applied to the quasi-steady mass and energy equations, Eqs. (A6)–(A8), to obtain *explicit* relations for droplet temperature and size (switching from droplet radius R to diameter D), as given in Eq. (25).

References

[1] Spalding, D. B., 1960, "A Standard Formulation of the Steady Convective Mass Transfer Problem," Int. J. Heat Mass Transfer, **1**(2–3), pp. 192–207.

[2] Kays, W. M., Crawford, M. E., and Weigand, B., 2013, *Convective Heat and Mass Transfer*, 4th ed., McGraw-Hill, New York.

[3] Mills, A. F., 2001, *Mass Transfer*, Prentice-Hall, Upper Saddle River, NJ.

[4] Lienhard, J. H., IV, and Lienhard, J. H., V, 2015, *A Heat Transfer Textbook*, 4th ed., Phlogiston Press, Cambridge, UK.

[5] Eckert, E. R. G., and Drake, R. M., Jr., 1959, *Heat and Mass Transfer*, McGraw-Hill, New York.

[6] Wang, K. T., and Brewster, M. Q., 2010, "Phase-Transition Radiation in Vapor Condensation Process," Int. Commun. Heat Mass Transfer, **37**(8), pp. 945–949.

[7] Moran, M. J., Shapiro, H. N., Boettner, D. D., and Bailey, M. B., 2014, *Fundamentals of Engineering Thermodynamics*, 8th ed., Wiley, New York.

[8] Brewster, M. Q., 2015, "Evaporation and Condensation of Water Mist/Cloud Droplets With Thermal Radiation," Int. J. Heat Mass Transfer, **88**, pp. 695–712.

[9] Bird, R. B., Stewart, W. E., and Lightfoot, E. N., 1960, *Transport Phenomena*, Wiley, New York.

[10] Incropera, F. P., DeWitt, D. P., Bergman, T. L., and Lavine, A. S., 2011, *Fundamentals of Heat and Mass Transfer*, 7th ed., Wiley, New York.